Supporting Information for:

Strong Axiality and Ising Exchange Interaction Suppress Zero-Field Tunneling of Magnetization of Asymmetric Dy_2 Single-Molecule Magnet

Yun-Nan Guo, Gong-Feng Xu, Wolfgang Wernsdorfer, Liviu Ungur, Yang Guo, Jinkui Tang, Hong-Jie Zhang,* Liviu F. Chibotaru,* and Annie K. Powell*

1 Synthetic procedures, Experimental techniques, structure and magnetic data

Synthetic procedures

All chemicals were of reagent grade and were used without any further purification.

Synthesis of compound 1

A red solution of $DyCl_3 \cdot 6H_2O$ (75.4 mg, 0.2 mmol) and the ligand pyridine-2-carboxylic acid [(2-hydroxy-3-methoxyphenyl)methylene] hydrazide (H_2**ovph**)[1] (54.2 mg, 0.2 mmol) in 15 mL of methanol/acetonitrile (1:2 v/v) was stirred for 5 min. Then, $NaHCO_3$ (33.6 mg, 0.4 mmol) was added and the reaction mixture was stirred for 3 h. The resultant yellow solution was left unperturbed to allow the slow evaporation of the solvent. Yellow single crystals, suitable for X-ray diffraction analysis, were formed after 3 days. Yield: 52 mg, (48%, based on the metal salt). Elemental analysis (%) calcd for $C_{33}H_{37}N_7O_9Cl_2Dy_2$: C, 36.99, H, 3.48, N, 9.15; found C, 36.37, H, 3.14, N, 8.81. IR (KBr, cm^{-1}): 3308 (br), 2830 (w), 1601 (s), 1553 (s), 1479 (s), 1344 (s), 1240 (m), 1216 (s), 1020 (m), 920 (w), 863 (w), 805 (s), 741 (s), 695 (m), 638 (m), 540 (w), 472 (m).

Crystal data for compound **1**: Monoclinic, space group $P2_1/c$, a = 9.6970(5), b = 29.0923(13), c = 13.9203(7) Å, β = 103.6050(10), V = 3816.8(3) $Å^3$, Z = 4, T = 186(2) K, D_{calcd} = 1.865 g cm^{-3}, R_{int} = 0.0519, 21026 reflections collected, $R_1(wR_2)$ = 0.0352 (0.0618) and S = 1.001 for 5370 observed reflections out of 7508 unique reflections with $I > 2\sigma(I)$. The data collection was performed using a Bruker APEX-II CCD, and the structure solution and refinement were carried out with SHELXTL.[2] CCDC−781817 contains the supplementary crystallographic data for this paper. These data can be obtained free of charge from the Cambridge Crystallographic Data Centre via www.ccdc.cam.ac.uk/data_request/cif.

Physical Measurements. Elemental analysis for C, H, and N were carried out on a Perkin-Elmer 2400 analyzer. FTIR spectra were recorded with a VERTEX 70 Fourier transform infrared spectrophotometer using the reflectance technique (4000–300 cm^{-1}). Samples were prepared as KBr disks. Magnetic susceptibility measurements were performed in the temperature range 2–300 K, using a Quantum Design MPMS XL-7 SQUID magnetometer equipped with a 7 T magnet. The dc measurements were collected from 2 to 300 K and the ac measurements were carried out in a 3.0 Oe ac field oscillating at various frequencies from 1 to 1500 Hz and with a zero dc field. The diamagnetic corrections for the compounds were estimated using Pascal's constants,[3] and magnetic data were corrected for diamagnetic contributions of the sample holder. Magnetization measurements on oriented single crystals were carried out with an array of micro-SQUIDs.

Crystallography. Suitable single crystal with dimensions of 0.17 × 0.15 × 0.12 mm^3 for **1** was selected for single-crystal X-ray diffraction analysis. Crystallographic data were collected at a temperature of 186 K on a Bruker ApexII CCD diffractometer with graphite monochromated Mo K_α radiation (λ = 0.71073 Å). The data processing was accomplished with the SAINT processing program.[4] The structure was solved by direct methods and refined on F^2 by full-matrix least squares using SHELXTL97.[2] The locations of the Dy atoms were easily determined, and Cl, O, N and C atoms were subsequently determined from the difference Fourier maps. All non-hydrogen

atoms were refined with anisotropic thermal parameters. The H atoms were introduced in calculated positions and refined with fixed geometry with respect to their carrier atoms.

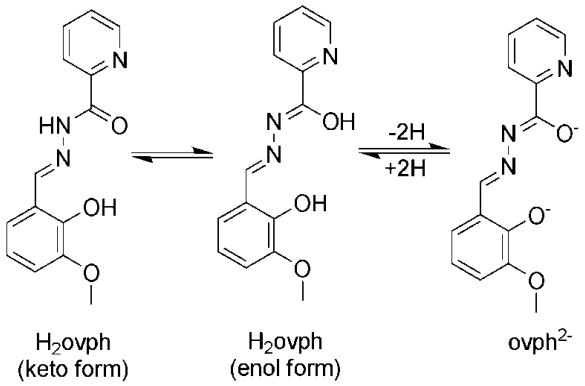

Scheme 1. The Keto-Enol tautomerism of the H_2ovph ligand and reversible deprotonation of its enolic form.

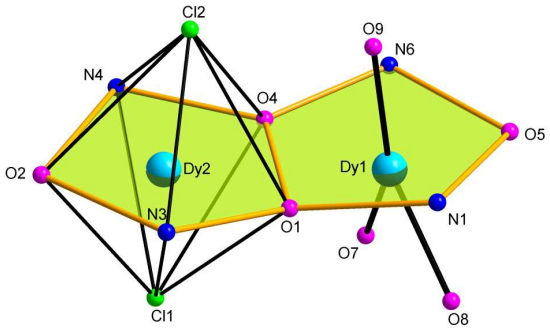

Figure S1. Coordination polyhedra observed in **1**: hula hoop-like geometry for Dy1 with the cyclic ring (hula hoop) is defined by the atoms N1, O1, O4, N6 and O5 and pentagonal bipyramidal environment for Dy2.

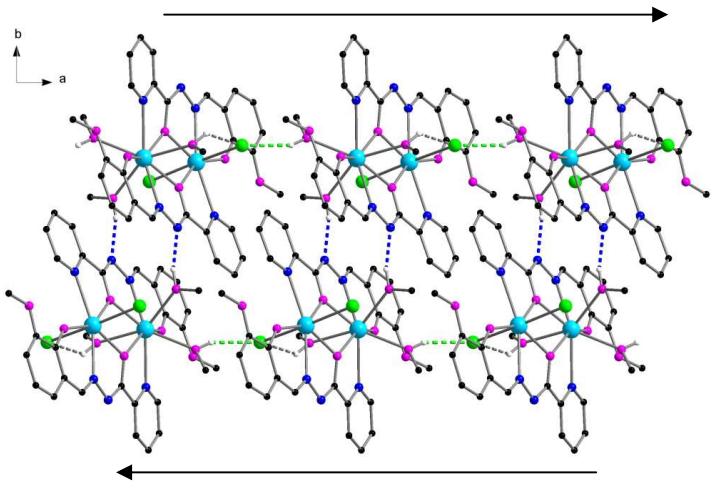

Figure S2. Illustration showing the hydrogen-bonding interactions (dash lines) in **1**, producing a 1D supramolecular chain with an anti-parallel arrangement of the molecules.

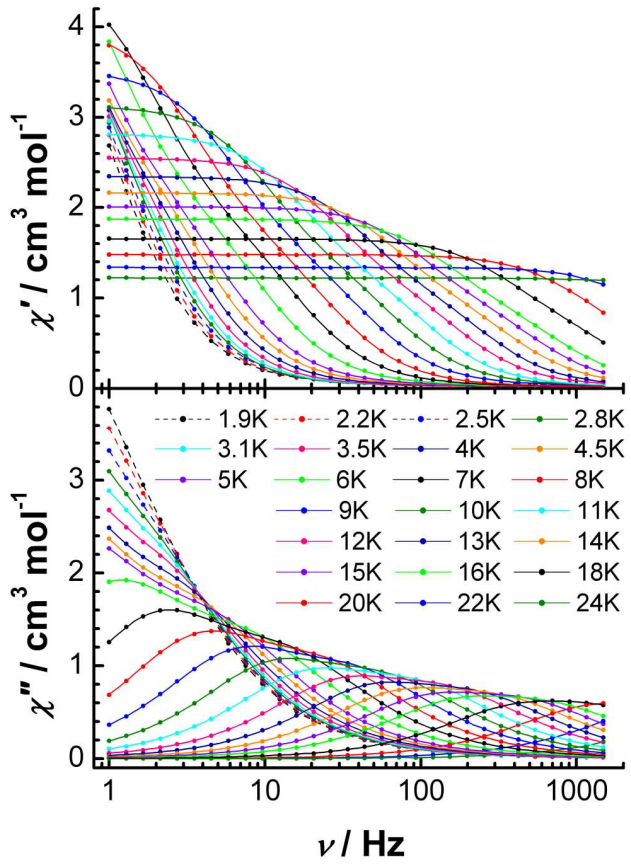

Figure S3. Frequency dependence of the in-phase (χ') and out-of-phase (χ'') parts of the ac susceptibility for **1**, measured between 1.9 and 24 K. The solid lines indicate the fits to eq. (1). The dashed lines are a guide for the eyes.

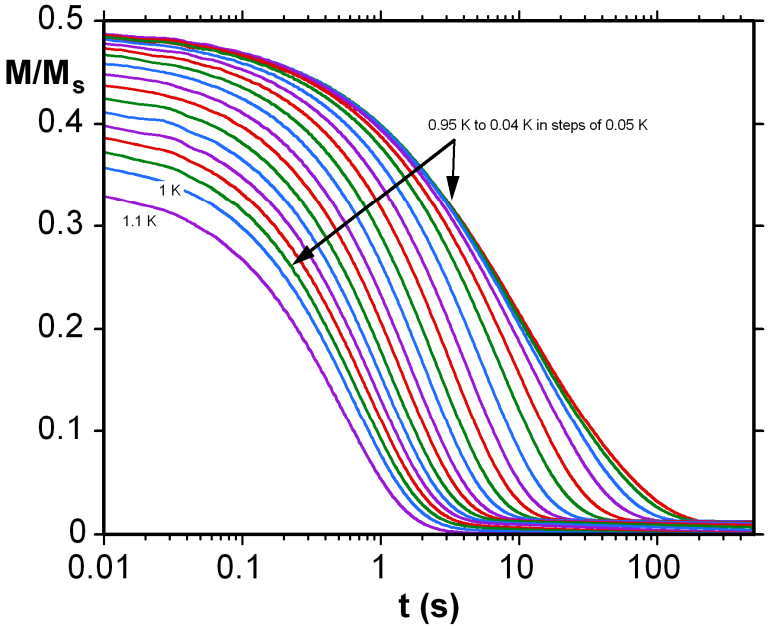

Figure S4. Magnetisation *vs.* time decay plots for a single crystal of **1** at the indicated temperatures.

2 Ab initio calculations for 1

Computational Details

The magnetic properties of metal centers in **1** have been studied by fragment *ab initio* calculations by using a specially designed routine SINGLE_ANISO[5] interfaced with the MOLCAS package.[6] In this connection, the question arises to cut suitable mononuclear fragments from the molecule, which would not change significantly the energy structure on the magnetic centre. To have a good description of the 4f ligand-field states within a fragment one needs to take into account the influence of the neighbouring metal ions. To this end the neighbouring Dy^{3+} have been simulated by an all-electron relativistic basis set for closed shell La^{3+}.

The second approximation concerned the coordination sphere. In order not to introduce additional errors, the full molecular structure was employed. No geometry optimization on the fragments have been done, all atomic coordinates being taken from the crystal X-ray analysis. The basis sets used for the calculations were taken from ANO-RCC basis libraries from MOLCAS package.[7]

For the electronic structure, the *ab initio* calculations were performed by means of MOLCAS-7.4 program.[6]

The active space of the complete active space self-consisting field (CASSCF) of calculation of the Dy included the 4f orbitals (CAS (9 in 7) since we are interested in the ligand field states only. The 4f orbitals are known to be localized, which allows us to consider the charge transfer states much higher in energy, thus being not relevant for the magnetism. The number and free ion parentage of states mixed by spin-orbit interaction in RASSI are listed together with the fragment description below.

With the obtained spin-orbit multiplets, the powder susceptibility and the g-tensors for the lowest Kramers doublets of isolated fragments were further evaluated using the recently developed *ab initio* methodology.[5] The basis of this approach is to calculate *ab initio* all angular moment matrix elements and then all magnetic moment matrix elements on the relevant spin-orbit multiplets obtained in CASSCF/CASPT2 calculations. These matrix elements are used in a separate routine to calculate:

(i) Magnetic properties measured directly in experiment (temperature dependent Van Vleck susceptibility tensor and powder averaged function, field dependent magnetization for different temperatures and directions and the powder magnetization);

(ii) Parameters of magnetic spin Hamiltonians for different spin-orbit multiplets and groups of spin states, described by the corresponding pseudospin, (*g* tensors, zero-field splitting tensors).

In calculations of magnetic properties, all spin-orbit multiplets on the sites are usually taken into account, in particular, all ligand-field states in the case of transition metal ions. This is important for correct quantitative account of the effects of strong magnetic anisotropy and strong applied magnetic fields. Computationally, this routine (SINGLE_ANISO) was interfaced with MOLCAS-7.4 program.

For the simulation of magnetic properties of polynuclear complexes we used an approach combining the calculated magnetic properties of individual metal fragments (CASSCF /RASSI-SO + SINGLE_ANISO) with the description of anisotropic exchange interaction between metal sites. The simulations have been done with a specially designed routine POLY_ANISO[5]. Both programs were interfaced with the SINGLE_ANISO routine treating individual metal fragments.

This *ab initio* based methodology has already been successfully applied for the treatment of the effects of strong magnetic anisotropy in polynuclear transition metal complexes. Thus it allowed to explain the origin of non-magnetic ground state in Dy_3 triangles,[8] to understand the complex magnetism in mixed-valent $Co^{II}_3Co^{III}_4$ heptanuclear wheel, in particular, the lack of SMM behaviour in this compound,[9] to explain the unusual magnetism of single-chain magnets.[10]

CASSCF calculations of local electronic and magnetic properties of Dy fragments in 1

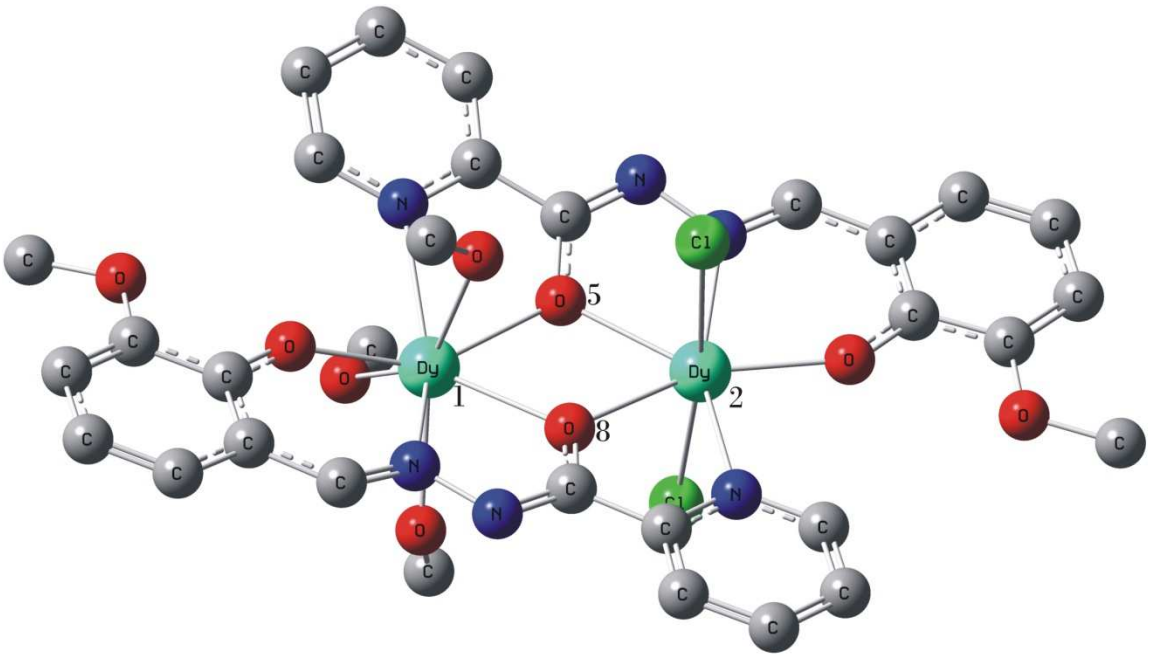

Figure S5. Molecular structure of **1**. Hydrogen atoms were not shown for clarity.

Since the dysprosium ions are structurally and chemically different, we employed two model fragments containing a single Dy ion. The structure of individual fragments is identical to the structure of the whole complex; the only difference is the substitution of the neighboring Dy ion with the diamagnetic La.

Computational details:

Basis Sets:

ANO-RCC [7s6p4d3f1g] – for Dy.

ANO-RCC [3s2p1d] – for close O and N.
ANO-RCC [3s2p] – for C and distant O and N.
ANO-RCC[4s3p1d] for Cl.
ANO-RCC [2s] – for H.

Active space:
CAS(9 in 7).

Roots mixed by spin-orbit coupling in RASSI:

In the best calculation all the states coming from the following multiplets have been taken into account in the spin-orbit interaction (RASSI): ^{6}H, ^{6}F, ^{6}P (all sextets), ^{4}I, ^{4}F, ^{4}M, ^{4}G, ^{4}L, ^{4}D, ^{4}H, ^{4}P, ^{4}G, ^{4}F, ^{4}I (128 out of 224 quartets), ^{2}L, ^{2}K, ^{2}P, ^{2}N, ^{2}F, ^{2}M, ^{2}H, ^{2}D, ^{2}G, ^{2}O (130 out of 490 doublets).

Table S1. Energies of the spin-free states and of the resulting spin-orbital multiplets (cm^{-1})

Spin multiplicity		Spin-Free states		Spin-orbital multiplets (Kramers doublets)	
		Dy1	Dy2	Dy1	Dy2
6	6H	0.000	0.000	0.000	0.000
		1.455	5.361	233.793	200.305
		332.452	297.487	316.992	415.152
		341.854	327.783	408.502	505.221
		390.383	548.733	491.700	555.745
		419.674	571.907	572.826	607.863
		615.058	582.132	609.456	680.781
		648.060	645.293	733.165	742.653
		653.674	771.067	3676.720	3650.864
		802.121	822.725	3787.812	3865.482
		813.816	882.856	3903.271	3950.030
	6F	7757.180	7777.990	3962.276	4024.953
		7840.972	7867.874	4030.561	4101.742
		7889.771	7920.196	4095.534	4151.796
		7926.594	7963.649	4196.123	4199.243
		7967.936	7997.905	6278.801	6271.595
		8007.696	8077.215	6334.680	6415.465
		8053.136	8115.363	6434.602	6468.431
	6P	34874.852	34825.512	6496.374	6541.521
		35161.237	35315.236	6571.305	6640.481
		35468.022	35437.699	6696.525	6719.046
4		24975.646	24966.278	8266.234	8277.869
		24977.794	24967.933	8315.536	8385.932
		25089.814	25119.283	8403.413	8433.991
		25103.440	25140.729	8490.803	8539.923

		25136.049	25151.817	8621.944	8657.047
		25171.129	25172.307	9800.898	9826.892
		25187.815	25178.685	9872.745	9924.862
		25253.922	25212.219	9968.495	10003.577
		25255.239	25246.373	10149.280	10188.823
		25278.796	25298.190	10215.433	10253.961
		…	…	10288.967	10286.908
2		37475.954	37489.321	10309.193	10360.183
		37476.767	37490.347	10326.883	10383.162
		37554.513	37554.388	10364.793	10425.624
		37558.858	37557.405	10407.352	10453.146
		37571.804	37576.329	10926.749	10950.969
		37592.694	37588.036	11153.612	11251.705
		37617.128	37641.069	11314.980	11320.624
		37652.569	37648.838	11698.489	11736.188
		37705.056	37742.244	11732.528	11769.611
		37714.054	37750.967	11743.833	11784.294
		…	…	…	…

Table S2. Main values of the *g* tensor of the ground Kramers doublet.

Ground Kramers doublet	projection	Dy1	Dy2
1	gx	0.0008	0.0027
	gy	0.0018	0.0051
	gz	19.6668	19.6880

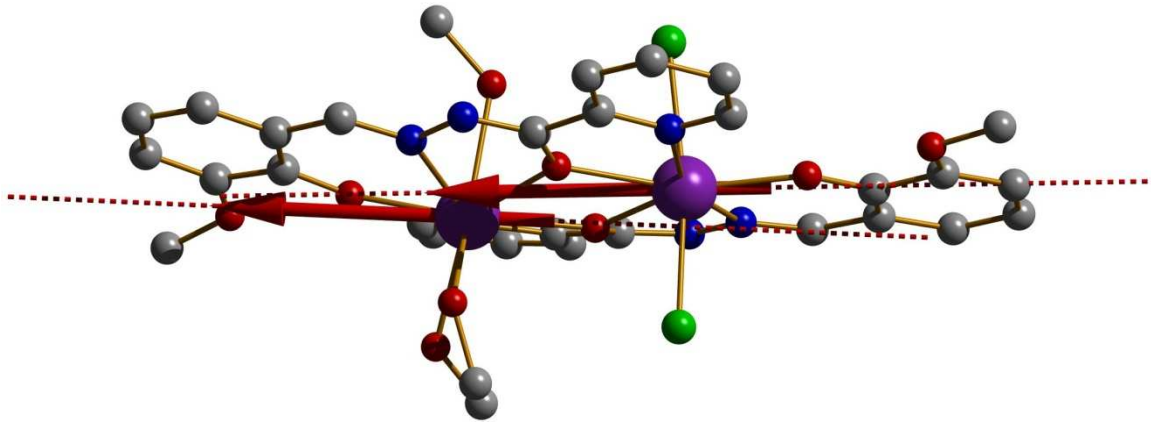

Figure S6. Orientations of local magnetic moments in **1**.

Relative orientations of the local magnetization if the ground state of **1** are shown in insert of Figure 3 and S6. Magnetic axes are almost parallel, lying almost in the plane formed by the two dysprosium ions and the one oxygen atom from the bridge connecting the Dy ions. These angles are shown in Table S3.

Table S3. Magneto-structural correlations for **1** (degrees).

	Dy1	Dy2
Angle between main anisotropy axes	8.79	
Angle of the main anisotropy axis with Dy-Dy axis	11.39	15.34
Angle formed by the main anisotropy axes with the Dy1-O5- Dy2 plane	7.13	1.08
Angle of the main anisotropy axis with the shortest bond on each Dy site	10.29	9.38

Calculations of the exchange spectrum and magnetic properties of 1

Exchange interaction between magnetic centers in **1** was found (within the Lines model):

$J_{Dy\text{-}Dy} = 0.235$ cm^{-1}

which corresponds to $J = 5.88$ cm^{-1} for the interaction between two effective spins $s = 1/2$. This parameter was used in the calculation of the temperature dependence of magnetic susceptibility (Figure 2) and high-field magnetization at 1.9 K (Figure S7).

Main values of the g tensor of the ground and first excited Ising doublets for **1** are shown in Table S4 in main test. The main anisotropy axis of the ground Ising doublet of **1** lies in the plane formed by the main anisotropy axes on Dy sites, bisecting the angle formed by local anisotropy axes on Dy sites.

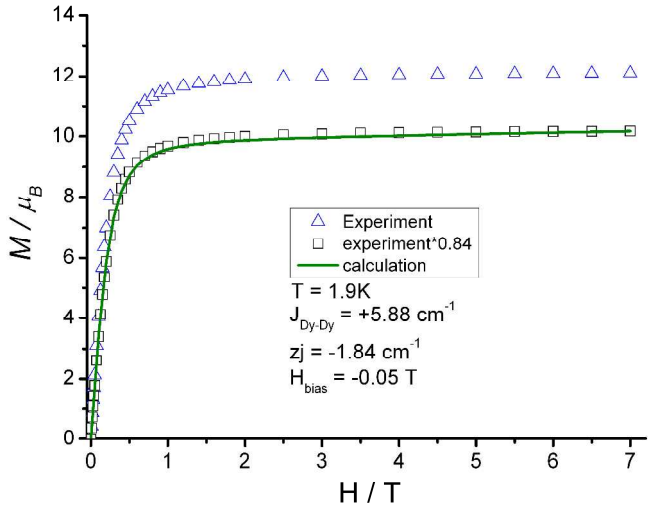

Figure S7. *M vs. H* data of **1** at 1.9 K. A comparison between experimental (empty triangles) and calculated (red line) powder molar magnetization at 1.9K of the Dy2 complex. The rescaled experiment with the coefficient 0.84 is shown by the empty squares. Each Dy^{III} ion is described as $S = 1/2$

Table S4. Main values of the *g* tensor of the ground and first excited Ising doublets for **1**.

Ising doublet	Energy (cm^{-1})	Tunneling splitting (cm^{-1})	*g* factors	Angle between g_z and Dy1-Dy2 axis
1	0.000000000 0.000000043	4.30×10^{-8}	$g_x=g_y=0$ $g_z=39.44$	12.8
2	2.850122199 2.850122290	9.10×10^{-8}	$g_x=g_y=0$ $g_z=3.04$	84.4
Angle between $g_z(1)$ and $g_z(2)$			90.4	

3 Two closely spaced relaxation processes in 1

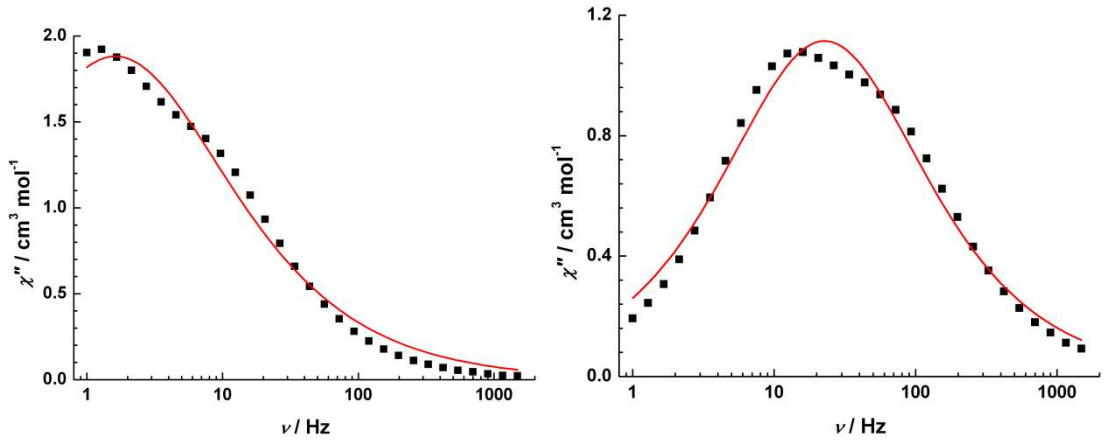

Figure S8. Out-of-phase (χ'') versus ν plots for **1** at 6K (left) and 10K (right). Solid lines: fits obtained with the following expression:[11]

$$\chi''(\omega) = (\chi_T - \chi_S)\frac{1+(\omega\tau)^{1-\alpha}\cos(\pi\alpha/2)}{1+(\omega\tau)^{1-\alpha}\sin(\pi\alpha/2)+(\omega\tau)^{(2-2\alpha)}}, \omega = 2\pi\nu$$

As seen from the fit above, the curves cannot be fit well, indicating there is more than one relaxation process.

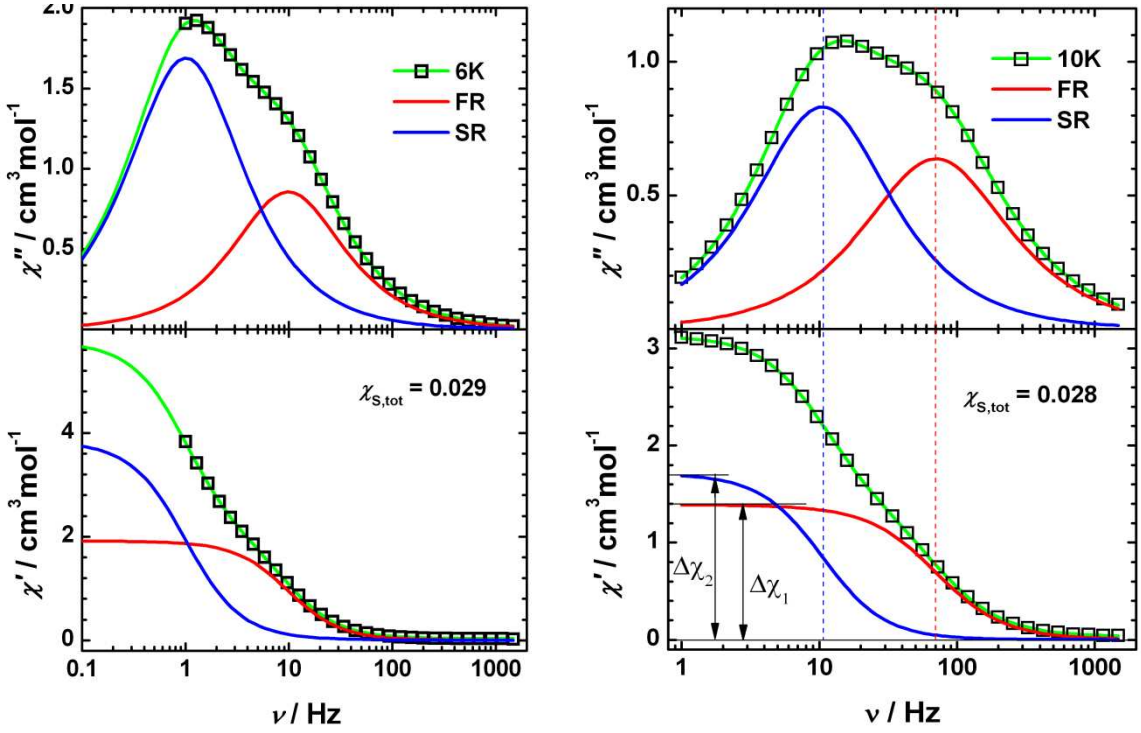

Figure S9. Resolution of χ' and χ'' *vs*. frequency curves at 6 K and 10 K. Red and blue lines correspond to FR and SR, respectively.

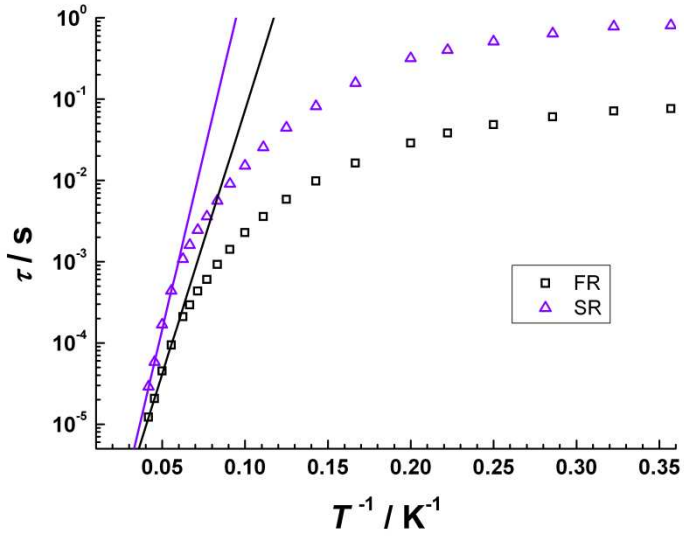

Complexes	U_{eff} / K	τ_0 / s	τ_{QTM} / ms
$[Dy_2(hmi)_2(NO_3)_2(MeOH)_2]$[12]	56	3×10^{-7}	3
$[Dy_2(hmi)_2(NO_3)_2(MeOH)_2]_\infty \cdot MeCN$[12]	71	7×10^{-8}	12
$[Cp_2Dy(\mu\text{-bta})]_2$[13]	56.6	1×10^{-7}	0.7
$[Dy_2(HBpz_3)_4(\mu\text{-ox})] \cdot 2CH_3CN \cdot CH_2Cl_2$[14]	42	---	8.2
$[Dy_2(hfac)_6(H2O)_4pz] \cdot 2pz$[15]	110	8.4×10^{-10}	3.5
$Dy_2(valdien)_2(NO_3)_2$[16]	76	6.04×10^{-7}	70
$[((Me_3Si)_2N)_2(THF)Dy]_2(\mu\text{-}\eta^2\text{:}\eta^2\text{-}N_2^{2-})$	26.1	2×10^{-6}	1.4
$[K(18\text{-crown-6})] \cdot [((Me_3Si)_2N)_2(THF)Dy]_2(\mu\text{-}\eta^2\text{:}\eta^2\text{-}N_2^{3-})$	178.1	8×10^{-9}	---
$[Dy_2$**ovph**$_2Cl_2(MeOH)_3] \cdot MeCN$ (this work)	150	2.3×10^{-8}	35000
	198	7.3×10^{-9}	

Figure S10. Magnetization relaxation time (τ) *vs.* T^{-1} plot for **1** obtained from the SR and the FR (Table S1), respectively. The dashed lines represent the best fits to the Arrhenius law of the thermally-activated region with the parameters given in the text. Table below the Figure shows the calculated observed barrier U_{eff} and pre-exponential factor τ_0, and tunneling rate τ_{QTM} – for the Arrhenius plot of **1**, and comparison with previously reported values in other Dy_2 SMMs.[17]

Table S5. Relaxation Fitting Parameters from Least-Squares Fitting of $\chi(\omega)$ data

		FR			SR		
T	$\chi_{S,\,tot}$	$\Delta\chi_1$	α_1	τ_1	$\Delta\chi_2$	α_2	τ_2
2.8	0.0322	2.826	0.050	0.0762	10.14	0.072	0.802
3.1	0.0311	3.015	0.059	0.0708	8.964	0.040	0.778
3.5	0.0286	2.850	0.062	0.0601	7.343	0.046	0.638
4	0.0268	2.690	0.068	0.0482	6.094	0.002	0.506
4.5	0.0253	2.556	0.074	0.0381	5.252	0.040	0.399
5	0.0257	2.239	0.070	0.0287	4.963	0.083	0.316
6	0.0282	1.897	0.066	0.0162	3.857	0.084	0.158
7	0.0274	1.820	0.070	9.82E-03	2.888	0.047	0.0816
8	0.0183	1.633	0.061	5.82E-03	2.383	0.039	0.0442
9	0.0294	1.485	0.055	3.58E-03	2.008	0.028	0.0254
10	0.0287	1.390	0.055	2.27E-03	1.709	0.018	0.0151
11	0.0313	1.241	0.043	1.41E-03	1.541	0.017	9.02E-03
12	0.0268	1.179	0.050	9.21E-04	1.341	0.010	5.60E-03
13	0.0272	1.067	0.034	6.00E-04	1.248	0.009	3.57E-03
14	0.0227	1.079	0.060	4.34E-04	1.060	0	2.43E-03
15	0.0375	0.958	0.037	2.93E-04	1.013	0.004	1.59E-03
16	0.0197	0.960	0.062	2.09E-04	0.894	0.003	1.07E-03
18	0.0044	0.808	0.033	9.42E-05	0.808	0.017	4.36E-04
20	0[a]	0.731	0	4.52E-05	0.750	0.017	1.67E-04
22	0[a]	0.701	0	2.16E-05	0.644	0.020	6.00E-05
24	0[a]	0.933	0	1.22E-05	0.289	0	2.90E-05

[a] These parameter values were fixed to 0.

4 Calculation of the magnetic susceptibility and the molar magnetization in the presence of intermolecular exchange interaction

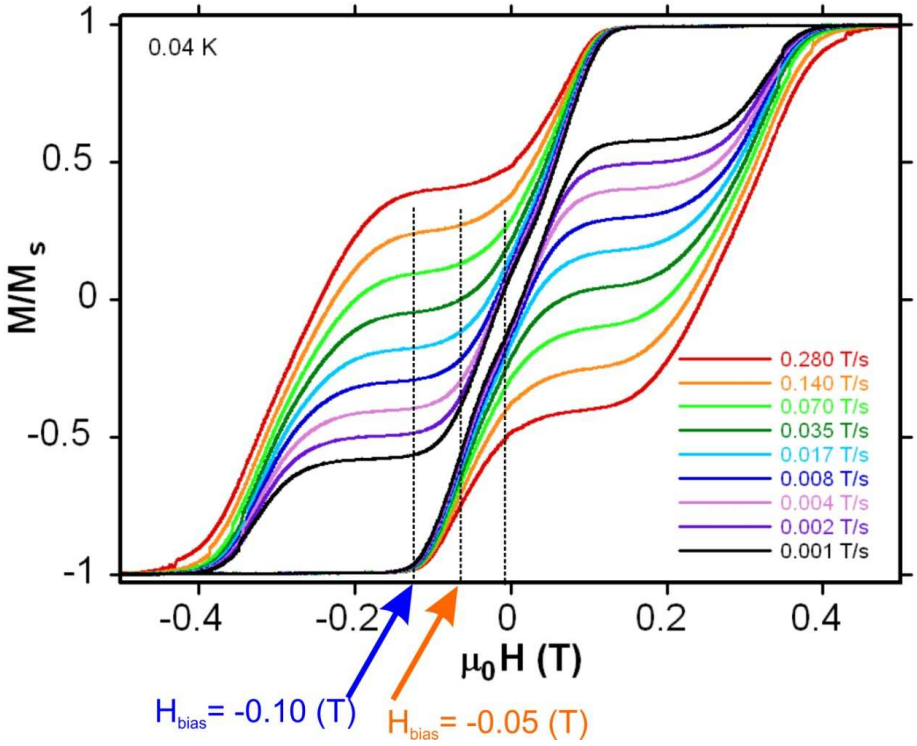

$$H_{bias} = \frac{zJ\langle S_{complex}\rangle}{\mu_B g}$$

In our case:

$\langle S_{complex}\rangle = \frac{1}{2}$ (the ground doublet state of Dy_2)

$g = 39.444$

$$zJ = \frac{H_{bias}\mu_B g}{\langle S_{complex}\rangle} = \frac{-0.05(T)\times 0.466864(cm^{-1}/T)\times 39.444}{1/2} = -1.84(cm^{-1})$$

This value corresponds to the effective spin 1/2 describing the ground doublet of Dy_2. In the Lines model the exchange interaction is expressed via the spins of the ground term of Dy^{3+} ions (S_i=5/2). In the ferromagnetic ground state the magnetic moments on Dy sites are parallel to each other and the spin of the Lines model is S_{Lines} =2*5/2=5. Evaluation of zJ for S_{Lines}/(1/2)=10 gives:

$$zJ = \frac{-1.84(cm^{-1})}{10\times 10} = -0.0184(cm^{-1})$$

Calculation of the magnetic susceptibility for this value of zJ and refitted $J_{Dy\text{-}Dy}$ is shown below in

green (the red curves are the results corresponding to zJ=0):

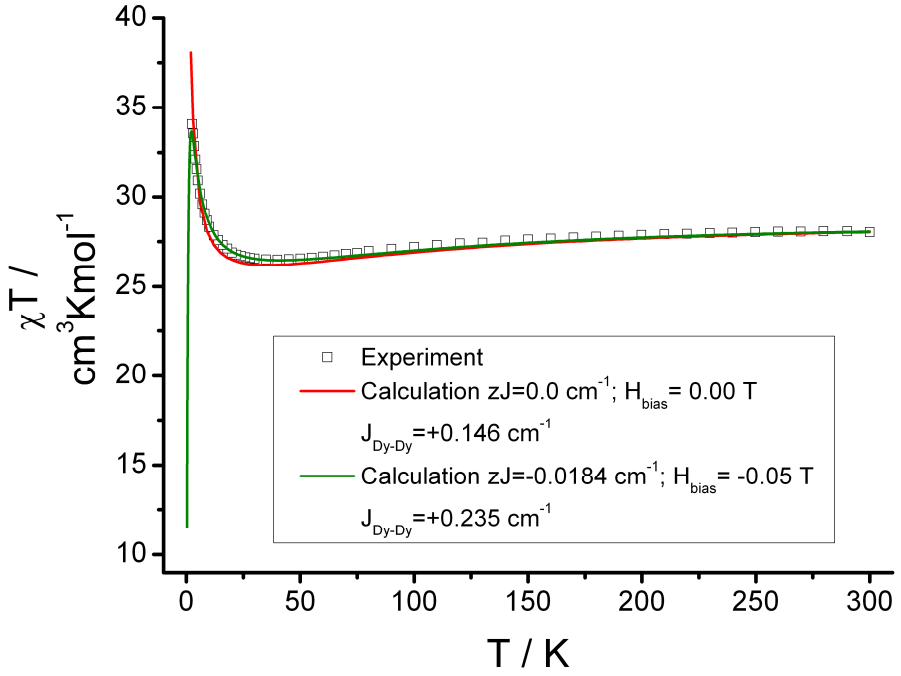

Figure S11. Magnetic susceptibility of **1** calculated for H_{bias}=-0.05 T.

For $H_{bias} = -0.10(T)$ the corresponding $zJ = -0.0368(cm^{-1})$

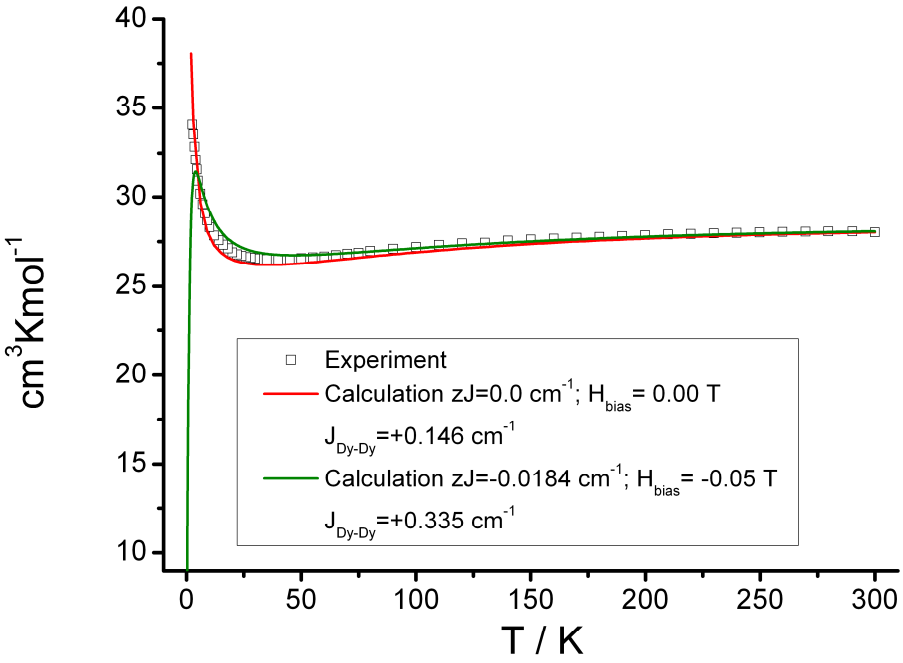

Figure S12. Magnetic susceptibility of **1** calculated for H_{bias}=-0.1 T.

The magnetization for these parameters is shown below:

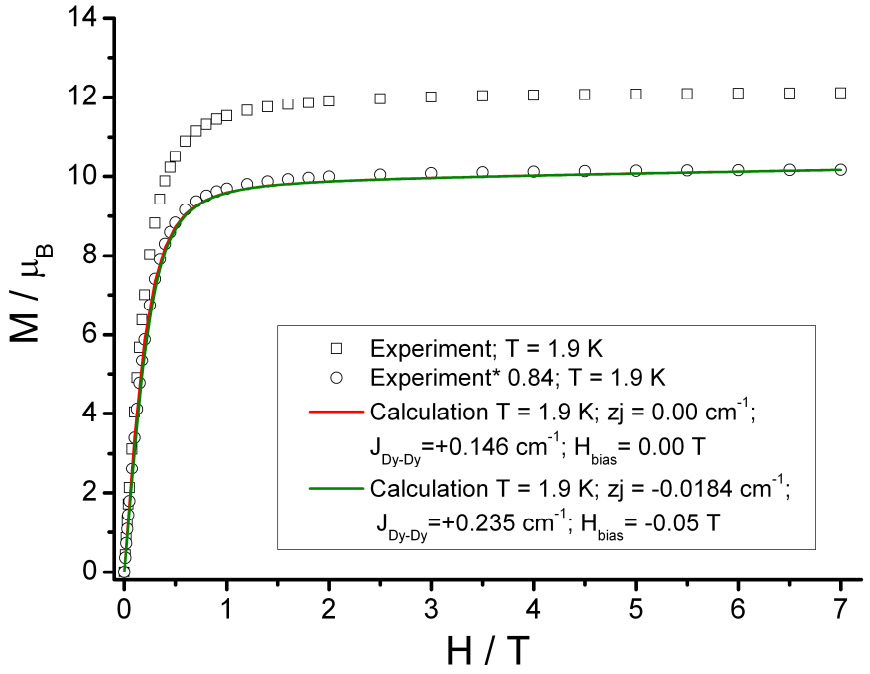

Figure S13. Magnetizatio of **1** calculated for H_{bias}=-0.05 T.

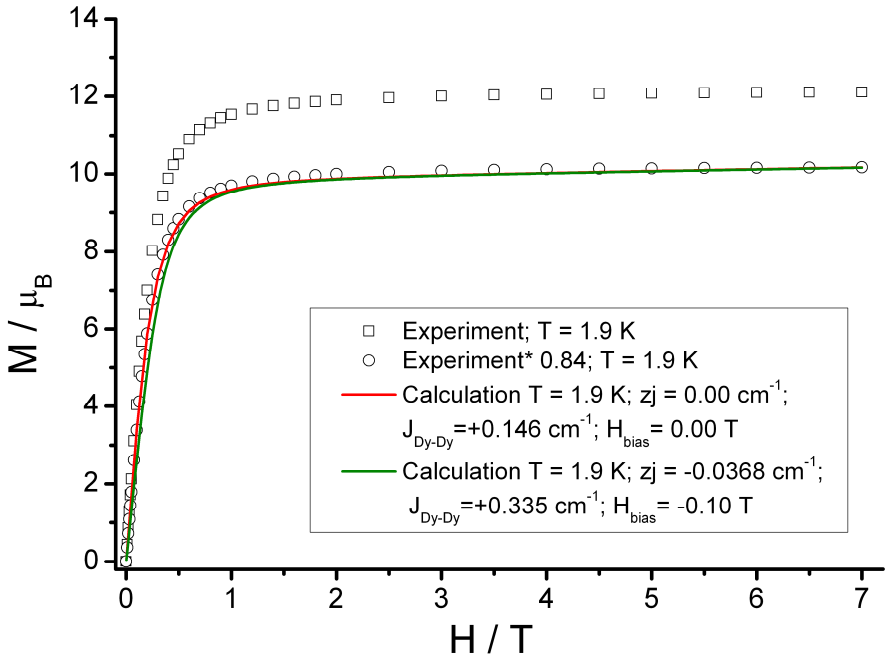

Figure S14. Magnetizatio of **1** calculated for H_{bias}=-0.1 T.

5 References

[1] D. Wang, S. X. Liu, *Polyhedron* **2007**, *26*, 5469.

[2] G. M. Sheldrick, *Acta Crystallogr. Sect. A: Found. Crystallogr.* **2008**, *64*, 112.

[3] *Theory and Applications of Molecular Paramagnetism*, Boudreaux, E. A. and Mulay, L. N. John Wiley & Sons, , New York, **1976**.

[4] *SAINT, Version 7.53a; Bruker Analytical X-ray Systems*, Madison.

[5] L. F. Chibotaru, L. Ungur, in *Programs SINGLE_ANISO and POLY_ANISO*, University of Leuven, **2006**.

[6] G. Karlstrom, R. Lindh, P. A. Malmqvist, B. O. Roos, U. Ryde, V. Veryazov, P. O. Widmark, M. Cossi, B. Schimmelpfennig, P. Neogrady, L. Seijo, *Comp. Mater. Sci.* **2003**, *28*, 222.

[7] B. O. Roos, K. Andersson, M. P. Fulscher, *Chem. Phys. Lett.* **1992**, *192*, 5.

[8] L. Ungur, W. Van den Heuvel, L. F. Chibotaru, *New J. Chem.* **2009**, *33*, 1224.

[9] L. F. Chibotaru, L. Ungur, C. Aronica, H. Elmoll, G. Pilet, D. Luneau, *J. Am. Chem. Soc.* **2008**, *130*, 12445.

[10] D. Visinescu, A. M. Madalan, M. Andruh, C. Duhayon, J. P. Sutter, L. Ungur, W. Van den Heuvel, L. F. Chibotaru, *Chem.-Eur. J.* **2009**, *15*, 11808.

[11] S. M. J. Aubin, Z. Sun, L. Pardi, J. Krzystek, K. Folting, L.-C. Brunel, A. L. Rheingold, G. Christou, D. N. Hendrickson, *Inorg. Chem.* **1999**, *38*, 5329.

[12] P. H. Lin, T. J. Burchell, R. Clérac, M. Murugesu, *Angew. Chem., Int. Ed.* **2008**, *47*, 8848.

[13] R. A. Layfield, J. J. W. McDouall, S. A. Sulway, F. Tuna, D. Collison, R. E. P. Winpenny, *Chem.-Eur. J.* **2010**, *16*, 4442.

[14] G. F. Xu, Q. L. Wang, P. Gamez, Y. Ma, R. Clérac, J. K. Tang, S. P. Yan, P. Cheng, D. Z. Liao, *Chem. Commun.* **2010**, *46*, 1506.

[15] Y. Ma, G.-F. Xu, X. Yang, L.-C. Li, J. Tang, S.-P. Yan, P. Cheng, D.-Z. Liao, *Chem. Commun.* **2010**, 8264.

[16] J. Long, F. Habib, P.-H. Lin, I. Korobkov, G. Enright, L. Ungur, W. Wernsdorfer, L. F. Chibotaru, M. Murugesu, *J. Am. Chem. Soc.* **2011**, *133*, 5319.

[17] The authors are grateful for the suggestion from a referee.